

Chapter 6

Introduction

The chromium(III)/chromium(V) couple is attractive for use as a catalyst in oxo atom transfer chemistry.¹⁻³ The challenge is to render the chromium(V) corrole more reactive towards substrates, while at the same time retaining chromium(III) reactivity towards O₂. Previous experience with porphyrins has shown that bromination of a ligand often increases its reactivity.⁴⁻⁹ As we have shown in the previous chapter, increase of reactivity should be linear with increase in bromination and therefore the maximum effect should occur at maximum bromination. Moreover, the fully brominated compound is also easier to isolate, which is a definite advantage. The main interest in work with a fully brominated compound was centered on two factors: reactivity towards substrate, and reactivity towards oxygen. The latter is more critical, since it is expected to decrease as the reactivity towards a substrate is increased.

From our work on the non-brominated compound, we already know that the rate of reoxidation is limited by the availability of a more reactive five-coordinate intermediate, which is in equilibrium with the six-coordinate complex through ligand dissociation.¹⁰ One of the main goals was therefore to examine how the ligand dissociation is affected by the increase in bromination and how it affects the overall rate of reoxidation. Of special interest were means of increasing the availability of the five-coordinate intermediate, through shifting of the dissociation equilibrium, since the reactivity of this species is expected to be much lower in the brominated compound, and therefore its availability might have to be increased if one expects any success at reoxidizing the brominated compound with oxygen. We show that the reactivity of **7** is increased to an extent that allows for epoxidation of olefins, while **8** is still reactive enough for activation

of O₂. The increase in reactivity in moving from **2** to **7** was quantified by electrochemistry and from the kinetics of their stoichiometric oxygen atom transfer to triphenyl phosphine.

Experimental

Materials

All chemicals were purchased either from Aldrich or EM science (solvents) and used as received except where otherwise specified. 4-methoxystyrene was purified by passing it through a small column of basic alumina before use. TFA was purified by distilling it from sulfuric acid (H₂SO₄/FA 1:10), followed by distillation from silver trifluoroacetate and addition of a small amount of trifluoroacetic anhydride (1% vol).

Preparation of (Br₈tpfc)Cr(py)₂, (**8**)

A mixture of **2** (24 mg, 0.03 mmol) and NBS (213.6 mg, 1.2 mmol) in methanol (50 mL) was heated to reflux for 4 hours, during which the color changed from deep red to dark emerald green. After solvent removal, the residue was purified on silica gel starting with a 1:1 mixture of hexanes/CH₂Cl₂ (yellowish reddish band). Switching to hexanes/CH₂Cl₂ (1:2) yielded a green band which was recrystallized from CH₂Cl₂ containing a few drops of pyridine. 31.1 mg (71.8 % yield) of a dark green powder were obtained. ESI-MS (MeOH): m/z (% intensity) 1507 (100 %) [M-2pyr + MeO]. UV-Vis (toluene), λ_{max} (ε•10⁻³ [M⁻¹cm⁻¹]): 350 (22.0), 392 (37.8), 420 (38.6), 444 (50.0), 490 (52.0), 550 (9.2), 578 (9.8), 624 (20.4), 658 (17.2) nm.

Preparation of (Br₈tpfc)Cr(O) (**7**)

a) via *m*-CPBA oxidation of **8**: A solution of **8** (10 mg 6.7 μmol) in methylene chloride. (5 mL) was treated with *m*-CPBA (11.6 mg 67 μmol). Addition of MnO₂ (to

destroy excess peracid) after 10 minutes and filtration yielded a red-brown solution. Such solutions were used directly, without attempting to isolate or further purify the compound. ESI-MS (MeOH): m/z (% intensity): 1492 (100%) [M]. UV-Vis (toluene) λ_{max} (relative absorbance): 424 (100) 584 (19.4). b) via aerobic oxidation of **8**: This route was used to prepare dilute solutions of **7** (<10 mM). The required amount of **8** was dissolved in toluene and heated to 80 °C for several hours in a closed vial. The color changed from green to orange-red, accompanied by the corresponding changes in the electronic spectrum.

Preparation of (Br₈tpfc)Cr(OPPh₃)₂ (9**)**

This compound was prepared via ligand exchange: A small amount of **8** (about 10 mM) was dissolved in a 1 mM OPPh₃ solution in toluene and left for half an hour.

Oxidation of PPh₃ by (Br₈tpfc)Cr(O) (7**)**

This fast reaction was monitored by stopped-flow techniques. One syringe was filled with an acetonitrile solution of accurate concentration of PPh₃ (in the range of 1-8 mM), and the other one with a dilute solution of **7** (~ 10 mM) in the same solvent. Equal amounts of both syringes were rapidly mixed and the time-dependent absorbances at 472 nm were used for data analysis. Five different PPh₃ concentrations were examined for determining the second-order rate constant.

Oxidation of 4-substituted styrenes by (Br₈tpfc)Cr(O) (7**)**

Certain aliquots of 4-substituted styrene (400-800 mL) were added to a stock solution of **7** in toluene, and the total volume was adjusted to 2 mL. The transformation of **7** to the corresponding chromium(III) complex was followed by monitoring the spectral changes at 424 (reagent) and 490 (product) nm. For product determination, a different procedure

was used. 30 mg (18.35 μmol) of **8** were dissolved in 1 mL CHCl_3 , followed by addition of an *m*-CPBA solution (3-6 mg in 5 mL) in the same solvent (200 mL). After 10 minutes the color change to red-brown was complete, and the mixture was passed through a small column of MnO_2 (5 x 0.5 cm) to destroy excess peroxide. The flask was washed with more solvent, the washings passed through MnO_2 (5 x 0.5 cm) and added to the rest of the solution as to adjust the total volume to 3 mL. One mL of that solution was diluted with another mL of solvent and 100 μL styrene was added and the solution was stirred until it turned back to green. The products were then analyzed by GC-MS. A blank sample was prepared using the same procedure, except that the solution of **7** was replaced by neat CHCl_3 .

Aerobic oxidation of $(\text{Br}_8\text{tpfc})\text{Cr}(\text{py})_2$ (8**) to **7****

A fresh toluene solution of **8** was divided into five 2 mL aliquots which were placed in sealed vials and heated at 80 $^\circ\text{C}$. A vial was removed every half hour, cooled down to room temperature, and its electronic spectrum was measured.

Reaction between $(\text{Br}_8\text{tpfc})\text{Cr}(\text{py})_2$ and TFA at low concentrations

A stock solution of **8** ($\sim 10 \mu\text{M}$ in pentane) as well as several solutions of TFA in the same solvent (different concentrations, range 0.1-1 mM) were prepared. 1 mL of solution containing **8** was placed in a cuvette and 1 mL of one of the TFA solutions was added, and a spectrum was taken every 10 s until full conversion. The measurements were repeated for each concentration and the data set for which resolution of both steps of the reaction was best was used to create the figures.

Reaction between (Br₈tpfc)Cr(py)₂ and TFA at high concentrations

TFA concentrations were chosen such a to make the first step of the reaction instantaneous on the experimental time scale. This allows the reaction's second step to be isolated. As above, stock solutions of **8** were prepared in pentane (~ 10 μM) as well as several solutions of TFA (1-10 mM). 1 mL of solutions of **8** placed in a cuvette and 1 mL of TFA/pentane solution was added and the traces monitored. Traces were fitted to a single-exponential, and the pseudo-first order rate constants were plotted against the TFA concentrations.

Preparation of pyridine-free/acid-free (Br₈tpfc)Cr(O)

A solution of **8** in pentane was treated with gaseous HCl for 30 s. An equal volume of water was added and the excess acid as well as the pyridinium salts were extracted. The layers were separated and the organic solvent was dried with magnesium sulfate, followed by filtration through a .3 μ filter. The solution was left to stand for 1 hour. UV-Vis measurements confirmed the formation of **7**.

Reactivity of pyridine-free/acid-free **7**

Stock solutions of **7** in pentane (~10 μM) were prepared by HCl treatment as described. Various solutions of 4-methoxystyrene were prepared in the same solvent (0.75-4.5 M). 1 mL of solutions of **7** was put in a quartz cuvette, and 1 mL of the styrene solution was added. The traces were monitored until completion of the reaction. The experiments were repeated with various concentrations of styrene.

As a control, pyridine was added to the stock solution of **7** previously used (114 μM final concentration). The controls were performed in the same ways as the experiments, using the same styrene solutions.

For product detection experiments, a more concentrated solution of **7** was prepared (0.23 mM) via acid treatment as described above. To 2.5 mL of this solution, 85 μ L of 4-methoxystyrene was added. A control was prepared by adding 85 μ L of 4-methoxystyrene to 2.5 mL of pentane. Both solutions were left to stand overnight at room temperature. An aliquot of each was then withdrawn and analyzed by GC-MS.

For inhibition studies, a 2mL pentane solution containing **7** (\sim 10 μ M) and 4-methoxystyrene (0.75 M) was put into a cuvette and its absorbance monitored for 5 hours.

Results and discussion

Bromination of **2** (synthesis of **8**, **9**, and **7**)

Bromination of **2** was achieved by treatment with a large excess of NBS (5 equivalents per hydrogen) in methanol. The new compound (**8**) is isolated as a trivalent bis-pyridine complex and shows an isotope pattern typical for eight bromines in its MS (Figure 6.1). There are no partially brominated compounds, which would be hard to separate. Similar to what was observed for [(tpfc)Cr^{III}(py)₂], **8** also can also exchange its pyridine ligands for OPPh₃, leading to **9**. Electronic spectra are non-isosbestic, pointing to the existence of a mixed-ligand intermediate during the process. The EPR spectrum of **8** is also typical for a chromium(III) complex, as shown in Figure 6.2b.

Oxidation of **8** by a peracid leads to **7**, which has the familiar Cr^VO d¹ EPR spectrum (Figure 6.2b). The transformation of **8** to **7** upon also occurs aerobically, but in a very slow process

Figure 6.1. ESI-MS of $(\text{Br}_8\text{tpfc})\text{Cr}(\text{py})_2$ in methanol. Main peak is $(\text{Br}_8\text{tpfc})\text{Cr}(\text{OMe})$.
Small peak is $(\text{Br}_8\text{tpfc})\text{Cr}(\text{O})$.

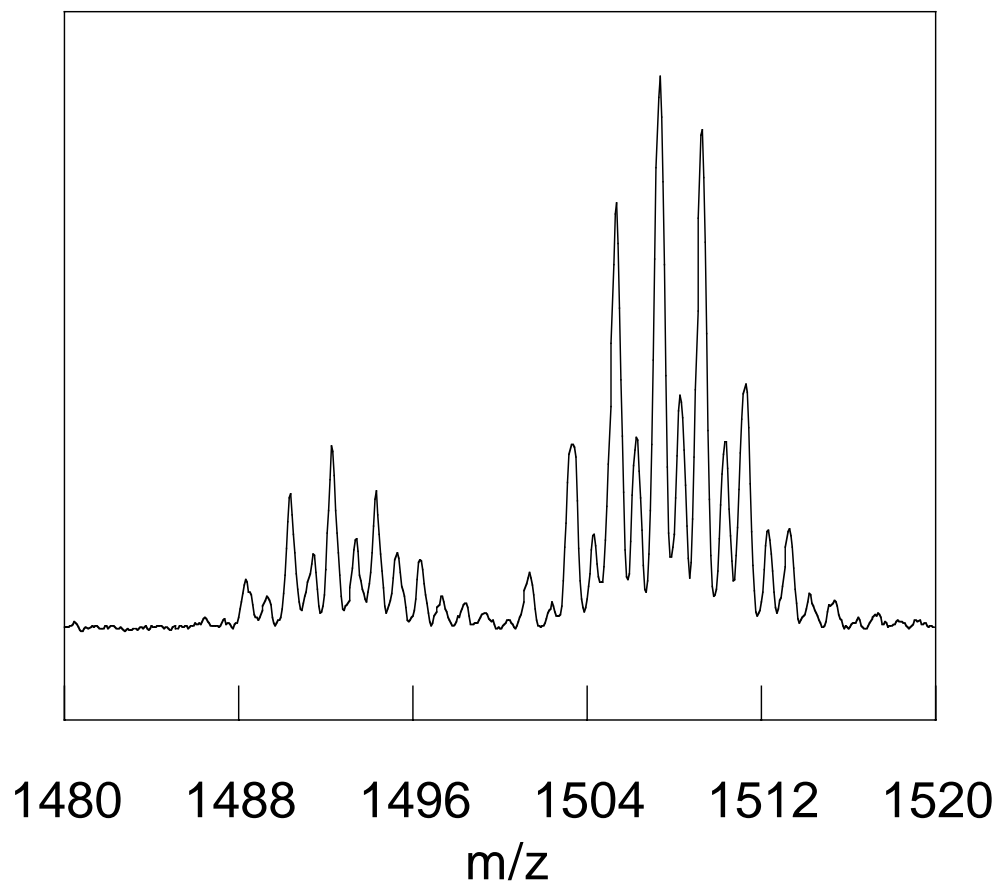


Figure 6.2a. UV-Vis spectra of $(\text{Br}_8\text{tpfc})\text{Cr}(\text{py})_2$ (solid line) and $(\text{Br}_8\text{tpfc})\text{Cr}(\text{OPPh}_3)_2$ (dashed line) in toluene.

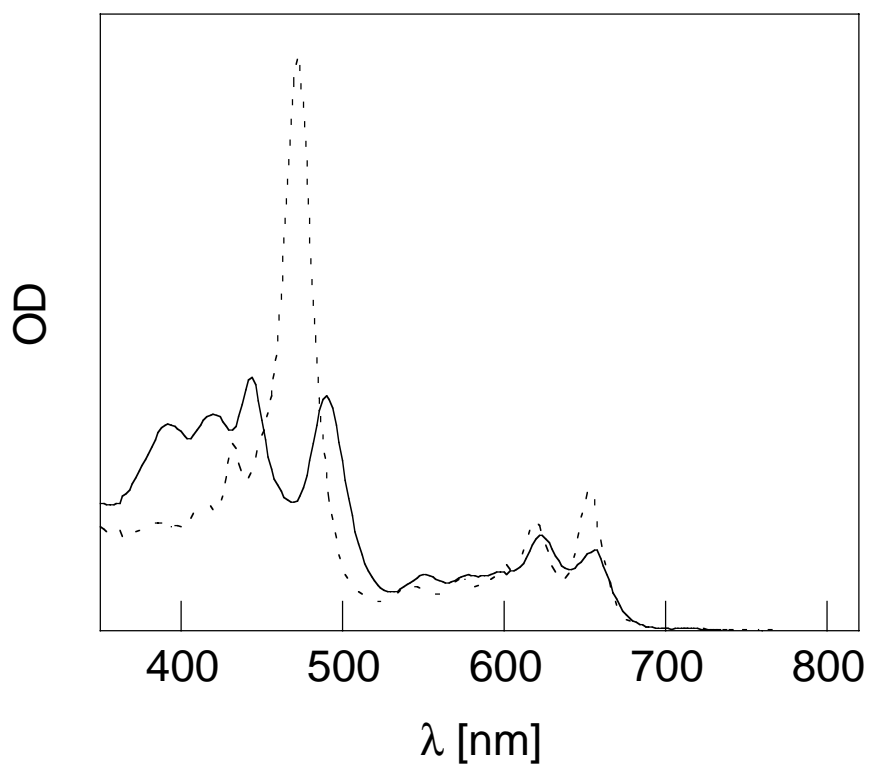


Figure 6.2b. EPR spectrum of $(\text{Br}_8\text{tpfc})\text{Cr}(\text{py})_2$ in pyridine/toluene 1:9. Inset: EPR of $(\text{Br}_8\text{tpfc})\text{Cr}(\text{O})$ in CH_2Cl_2 .

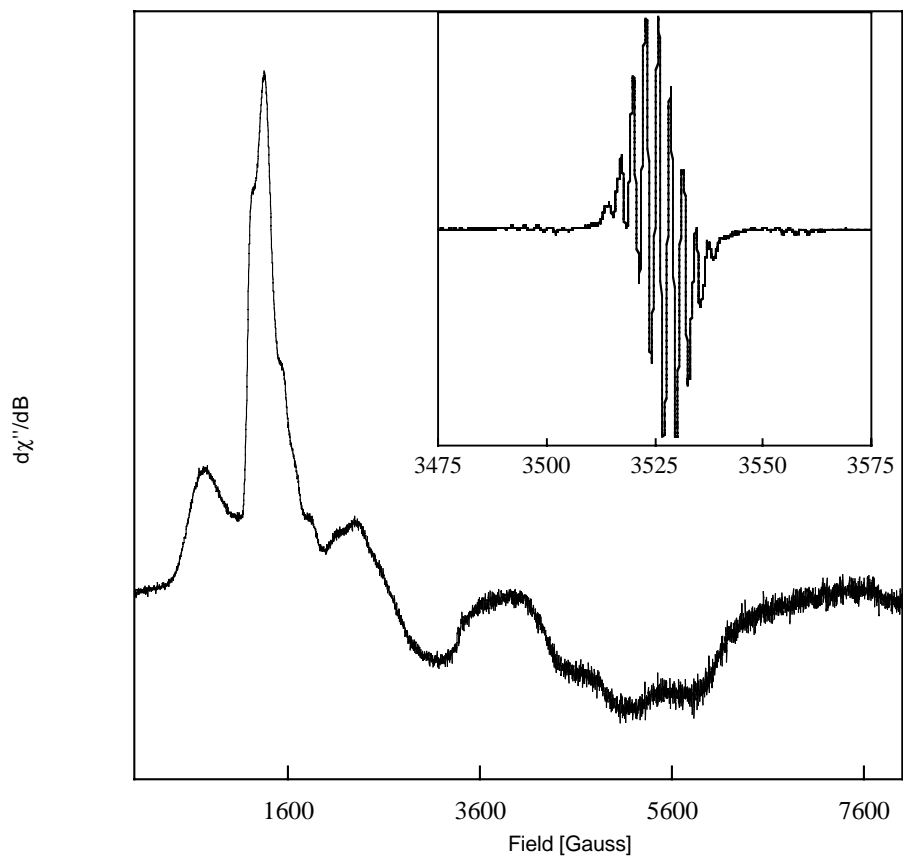


Table 6.1. EPR parameters for **2** and **7**.

	(tpfc)Cr(V)(O) (2)	(Br ₈ tpfc)Cr(V)(O)(7)
g_{iso}	1.986	1.982
$ a(^{53}\text{Cr}) $ (mT)	1.64	1.85
$ a(^{14}\text{N}) $ (mT)	0.30	0.28
$E_{1/2}^{\text{a}}$ (mV) (mV vs. Ag/AgCl)	110	578

^a Versus Ag/AgCl

(in the order of weeks for dilute (10 mM) solutions). Heating to 80 °C allows for effective oxygenation of **8** within a few hours.

Oxygen atom transfer from **7** to styrenes

a) Kinetics measurements: Only the brominated compound **7** is reactive towards styrene. The reaction follows pseudo-first-order kinetics in the presence of an excess of styrene and is first order in chromium as well. This is consistent with a bimolecular reaction between **7** and the olefin. The reactivity was found to increase with more electron –rich olefins, as shown in Table 6.1. With this limited series, the Hammett ρ value is -4.21 .

b) Stoichiometric oxidation: Two major oxidation products were found in the reaction of **7** with styrene, styrene oxide and phenylacetaldehyde, together with smaller amounts of benzaldehyde. Control experiment shows that benzaldehyde is formed by the interaction of styrene with air, and is therefore not due to the presence of the catalyst. Only the first two products, which are absent in the control, are due to reaction between **7** and styrene. The yields after subtraction of benzaldehyde formed via autooxidation were 20% styrene oxide and 10% phenylacetaldehyde.

Turning to substituent effects in the oxidation of styrenes, we see that there is a LFER between the oxidation potential of the olefin and its reactivity with **7**.

$$\log k_{obs} = -2.36 \log(E_{1/2}) - 0.49 \quad (1)$$

where $E_{1/2}$ values are taken from the previously mentioned paper¹¹. In porphyrins, the mechanism of oxo transfer from $\text{Cr}^{\text{V}}(\text{O})$ to olefins has been proposed to go through a charge-transfer complex between the olefin and the high-valent metal-oxo.^{11,12}

The slope obtained in equation (1) is similar to the one observed for $(\text{Br}_8\text{TPP})\text{Cr}^{\text{V}}(\text{O})$.¹¹ It is therefore likely that the mechanism is similar and we propose that in the case of oxidation of olefins by $(\text{Br}_8\text{TpFPC})\text{Cr}^{\text{V}}(\text{O})$ the transition state is also a charge-transfer complex. A concerted oxo transfer would then lead to the epoxide, whereas an electrophilic addition on one side of the olefin would likely result in rearrangement products.

Figure 6.3. Linear free energy plot for the reactivity of *para*-substituted styrenes in toluene in terms of the Hamett σ parameter.

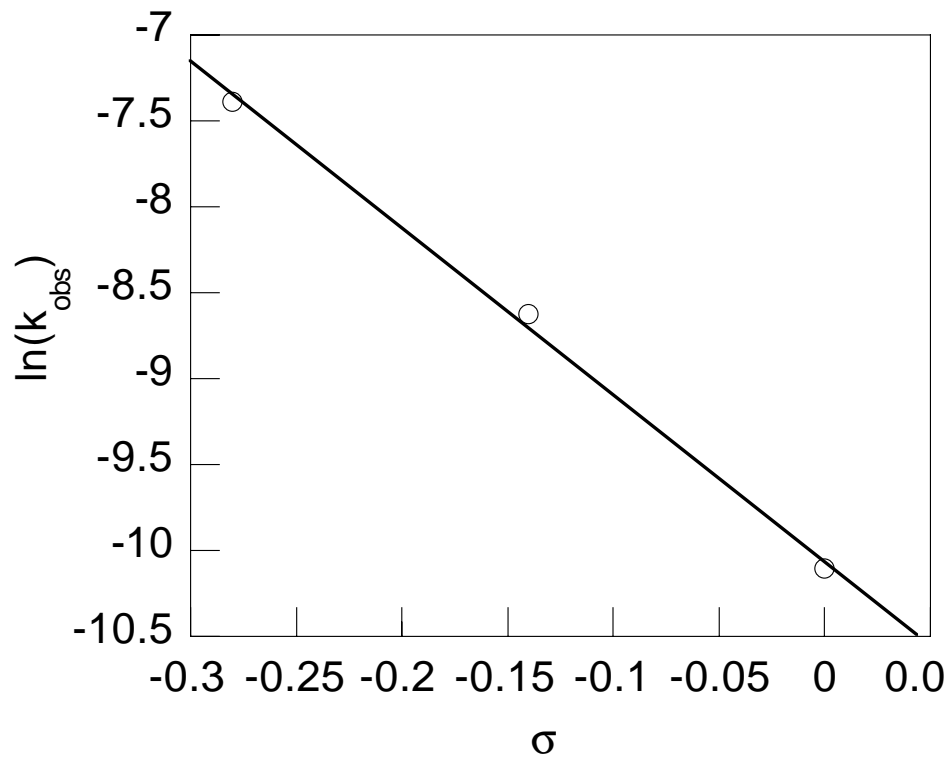


Table 6.2. Kinetic parameters for O-atom transfer to substrates in toluene.

	(tpfc)Cr(V)(O) (2)	(Br ₈ tpfc)Cr(V)(O) (7)
PPh ₃ (M ⁻¹ s ⁻¹)	9.2 ± 0.8	8.2 ± 0.3 • 10 ⁻³ ^a
<i>p</i> -MeOstyrene (M ⁻¹ s ⁻¹)	No reaction	62 ± 3 • 10 ⁻⁵
<i>p</i> -Mestyrene (M ⁻¹ s ⁻¹)	No reaction	18 ± 2 • 10 ⁻⁵
Styrene (M ⁻¹ s ⁻¹)	No reaction	4.1 ± 0.7 • 10 ⁻⁵

^a In CH₃CN

The CH-CBr substitution affects the EPR hyperfine couplings (increase of $|a(^{53}\text{Cr})|$, decrease of $|a(^{14}\text{N})|$ (Table 6.1)), as well as the redox potential of the $\text{Cr}^{\text{V/IV}}$ couple (positive shift of nearly 500 mV). The couplings in the EPR are an indirect measure of the diminished (N->Cr) s donation, which is critical in stabilizing the metal oxygen bond.¹³ We expect **7** to be more reactive than **2**. This can best be seen in the relative reactivity of **2** and **7** towards PPh_3 . The difference in rates corresponds to a decrease in activation energy upon bromination (**7** vs. **2**) of 3.99 kcal/mol). This may be compared with the 10.65 kcal/mol (corresponding to 460 mV shift) increase of the $\text{Cr}^{\text{V}}/\text{Cr}^{\text{IV}}$ oxidation potential in **7** relative to **2**. Accordingly **7** was also found to be reactive towards activated olefins, like styrenes. The reactivity is still below that of a porphyrin, which suggests that **7** is in between corroles and porphyrins, in terms of ligand σ donation as measured by the $\text{Cr}^{\text{V/IV}}$ potential and should behave in a way common to both in terms of reactivity.

This is particularly true if one turns to the reoxidation of the Cr^{III} state. There is no known case of a $\text{Cr}^{\text{V}}\text{O}$ porphyrin that is both able to transfer its oxygen atom to an olefin substrate and to be reoxidized by air. The $\text{Cr}^{\text{V}}\text{O}/\text{Cr}^{\text{III}}$ states take part in the oxygen atom transfer step, while the $\text{Cr}^{\text{IV}}\text{O}/\text{Cr}^{\text{II}}$ states are involved in aerobic reoxidation. However **7** seems to be able to reoxidize with air after oxygen atom transfer, although at an extremely slow rate, which makes it unsuitable for catalysis. By analogy, we also postulate that the complex has to go through a 5-coordinate intermediate before reoxidation can take place. As ligand dissociation in porphyrins becomes disfavored with increasing electronegativity of the ligand, bromination of the corrole works against

reoxidation by reducing the reactivity of the 5-coordinate intermediate, and limiting its availability through disfavoring dissociation of the axial pyridine.

Reoxidation of $(\text{Br}_8\text{-tpfc})\text{Cr}(\text{py})_2$ in the presence of TFA

The reoxidation of $(\text{Br}_8\text{tpfc})\text{Cr}(\text{py})_2$ is extremely slow. As noted above, this can be speeded up considerably by using higher temperatures. From the mechanistic information gathered on the parent compound $(\text{tpfc})\text{Cr}(\text{py})_2$ we know that axial ligand dissociation is a rate-limiting step. What is more, dissociation of axial ligands in porphyrins is known to become disfavored as the ring electron density diminishes. In corroles, this dissociation constant was found to be 45 μM for the non-brominated corrole with triphenylphosphine oxide as the ligand. Since nitrogen ligands are known to bind more tightly, the dissociation constant for axial pyridine is expected to be very low for the fully brominated compound. This adds to the low reactivity of this compound towards O_2 to render reoxidation extremely difficult. As pointed out in the preceding section, the only factor over which control can be exercised is the axial ligand dissociation constant. We decided to displace the equilibrium in favor of dissociation by trapping the free pyridine with an acid. We choose TFA, because its adduct with pyridine is well characterized.

Upon treating $(\text{Br}_8\text{tpfc})\text{Cr}(\text{py})_2$ with a small amount of TFA, a distinct change is observed in its UV-Vis spectrum. The transformation is typical of formation of $(\text{Br}_8\text{tpfc})\text{CrO}$ as final product. The absence of a clean isosbestic point, however, indicates the presence of an observable intermediate.

Closer examination of the traces shows the rapid (within 50 s) disappearance of the starting material, with formation of an intermediate, which then decays to the final $\text{Cr}^{\text{V}}\text{O}$ product in a few minutes (Figure 6.4). The spectrum of the intermediate is very similar to

that of the starting material, especially in the Q band region, which shows a series of four bands, similar to the starting material. From our work with the parent compound, we know that those bands are characteristic of a Cr^{III} state, since none of the higher oxidation states displays more than 2 Q bands. The only change is in the intensity of one of the two Soret bands, which is associated with a change in axial ligation. This shows that the intermediate is a Cr^{III} species with different axial ligation pattern, most likely a five-coordinate species (Figure 6.5). This species is a lot more reactive towards O₂ due in part to the presence of an open coordination site, and it is no surprise that this intermediate is rapidly converted to the final product.

Role of TFA during oxidation

As seen above, TFA allows for a displacement of the equilibrium towards dissociation of the axial pyridine. The next step was to ascertain whether TFA also played a role in the oxidation step itself. In that series of experiments, the TFA concentration was high enough so that ligand dissociation step was very rapid.

Figure 6.4. Absorbance traces at 502, 472, and 481 nm, showing the disappearance of **8**, appearance of an intermediate, and formation of **7**.

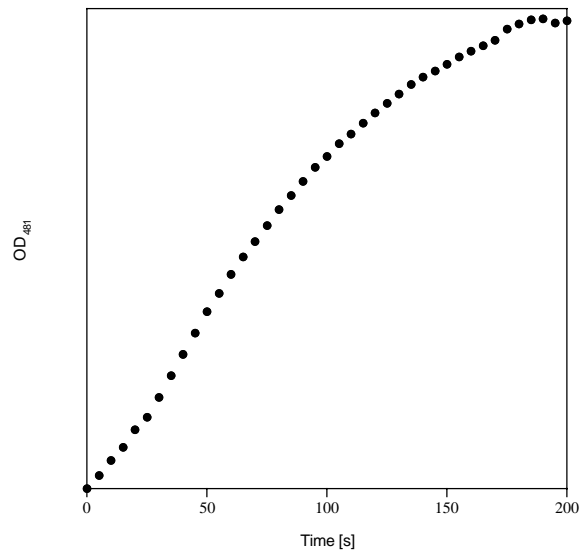
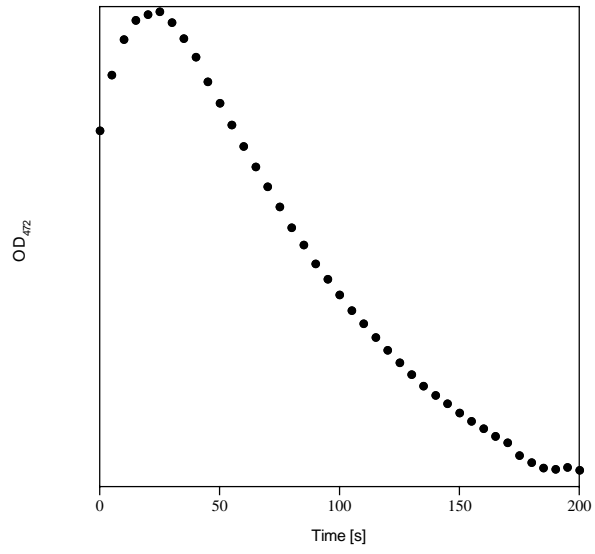
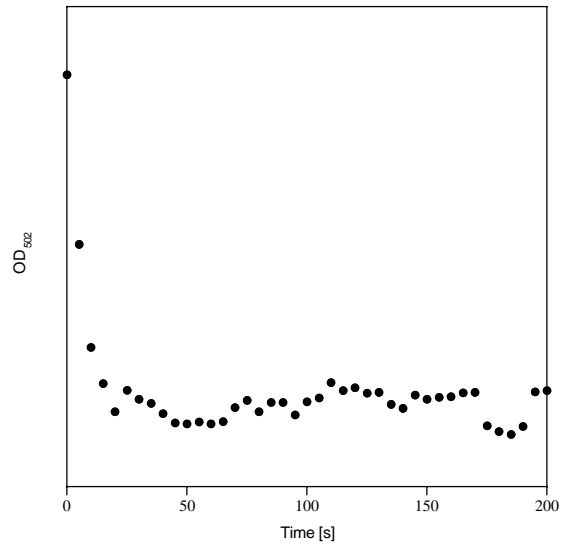
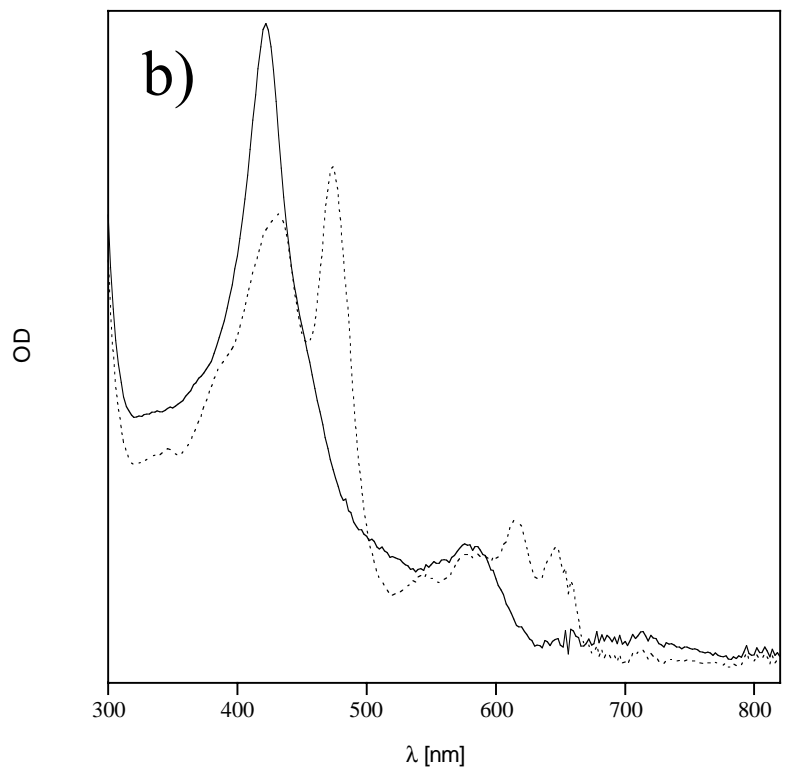
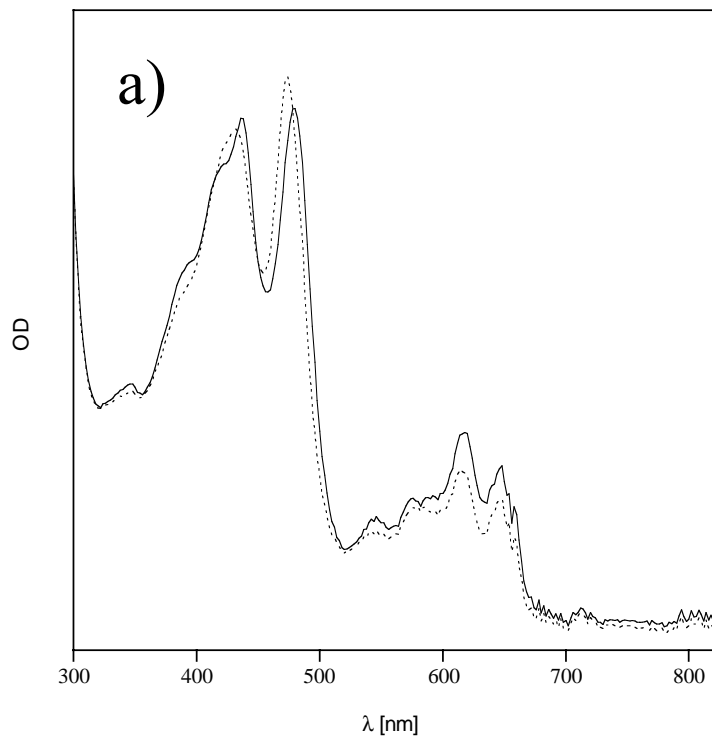


Figure 6.5. Comparison of the spectra of : a) **8** and intermediate in pentane. b) **7** and intermediate in pentane. The intermediate is always shown as a broken line.



Measuring the rate of reaction using different TFA concentrations, we see that there is a linear dependence of the rate of oxidation upon acid concentration (Figure 6.6). However, there is a clear nonzero intercept, which suggests the following experimental rate law:

$$k_{obs} = k_1 + k_2[TFA]$$

One interpretation of this is that the oxidation of the intermediate occurs via two pathways, one being acid dependent. TFA thus plays a non-innocent role in reoxidation of chromium corroles.

Preparation of pyridine-free (Br₈tpfc)Cr(O)

To examine the use of (Br₈tpfc)Cr(O) as a catalyst, we needed a system without pyridine, for the reasons outlined above. Also, since TFA is a participant in the reoxidation step, we wanted the possibility of removing the acid after pyridine trapping. We thus switched to a new approach, whereas HCl is used in its gaseous form to trap the pyridine as its pyridinium chloride salt. The salt, as well as any excess acid is then extracted using water, which is not miscible with the organic solvents used. The procedure yielded a pentane solution of **7** free of any axial ligand or acid, which provided us with the catalyst in a form ready for study.

Reactivity of (Br₈tpfc)Cr(O)

Having succeeded in preparing the complex in a ligand/acid free form, we wanted to examine its potential uses as a catalyst for olefin oxygenation. We chose 4-methoxystyrene as substrate, since it is readily available and more reactive than unsubstituted styrene. The experiment itself was based on the fact that in the absence of reoxidation of the catalyst, **7** decays to **8** in a simple monoexponential fashion. The

presence of significant reoxidation would manifest itself by a steady state, where the rate of reoxidation equals the rate of reaction with the substrate, i.e.:

UV-Vis measurements of a solution of **7** in pentane in the presence of methoxystyrene show that there is a rapid establishment of a steady state (within 200 s). The final spectra obtained are typical of a mixture of **7** and **8** (Figure 6.7). The ratio of **7** to **8** depends on the amount of methoxystyrene added. This behavior suggests that we are indeed observing catalytic turnover.

As a control, we repeated the experiment in the presence of a small (114 μM) amount of pyridine. In that case, the traces are different, **7** being totally converted into **8** in every case, with the kinetics following a pseudo-first order in styrene (Figure 6.8). In that case, the added pyridine effectively blocks the axial sites preventing oxidation. This suggests that in the absence of pyridine,

Figure 6.6. Dependence of the rate of oxidation of **8** in pentane upon the concentration of TFA.

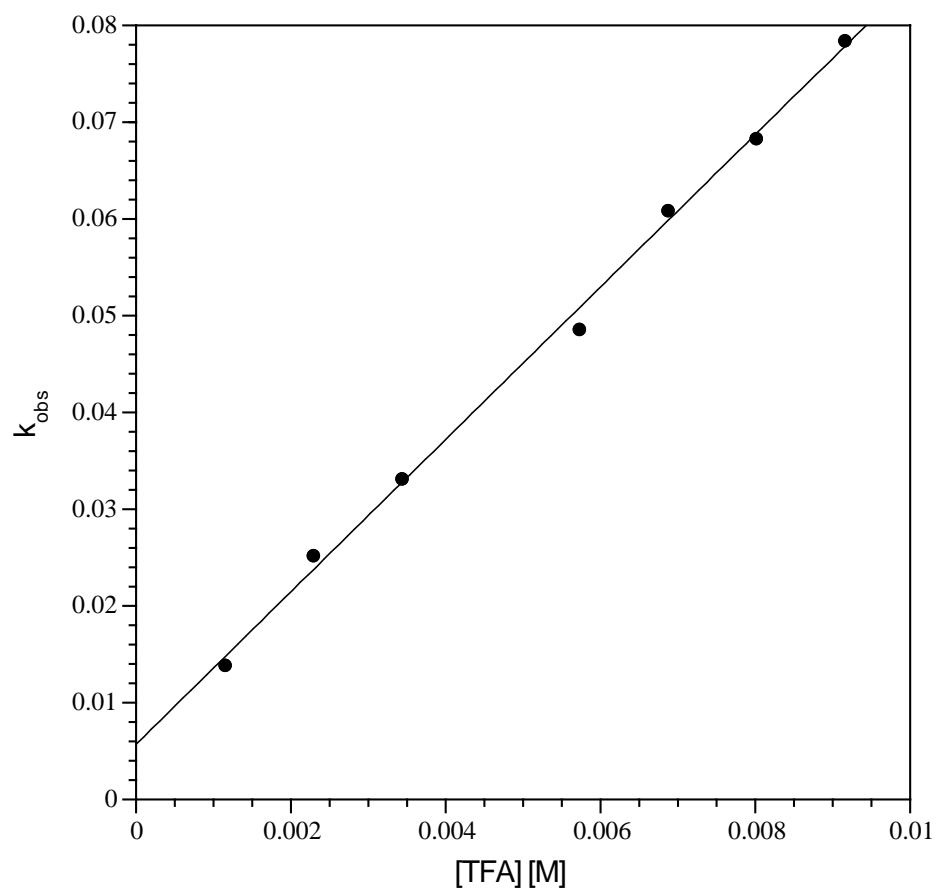
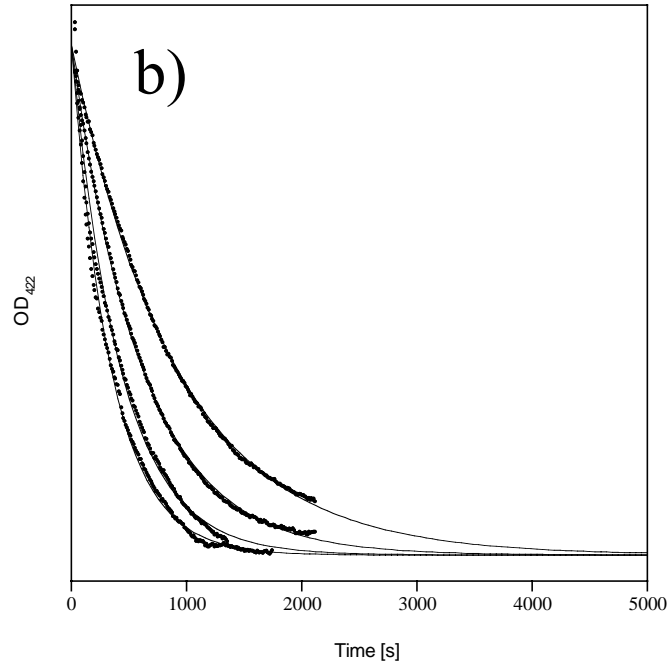
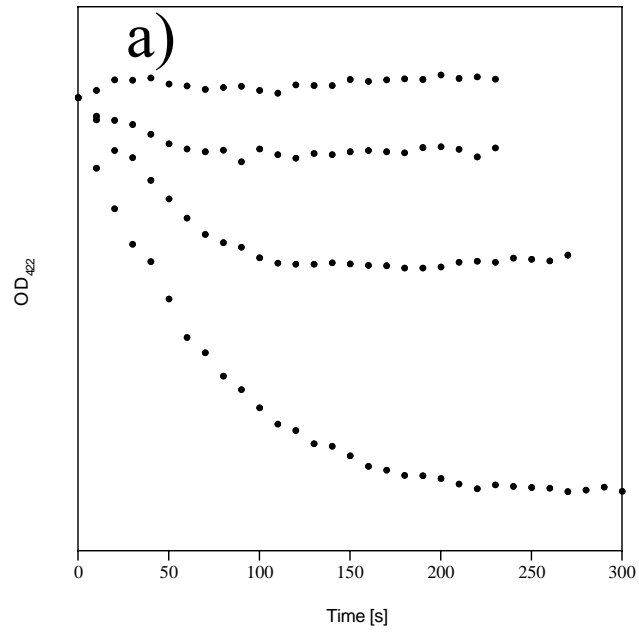


Figure 6.7. Typical traces for the reaction of **7** with increasing amounts of 4-methoxystyrene in the absence (a) and the presence (b) of pyridine.



reoxidation does indeed occur. Using the pseudo-first-order rate constant derived from the experiments done in the presence of pyridine, we were able to determine k_{ox} and found that:

$$k_{\text{ox}} = 5.74 \cdot 10^{-3} \text{ s}^{-1}$$

This value is close to the value obtained for the TFA-independent oxidation, which reinforces our hypothesis of reoxidation of the catalyst by O_2 .

As an additional proof of catalytic turnover, we did a scaled-up experiment, which allowed for analysis via GC-MS of the reaction mixture. In those experiments we generally noticed that the catalyst was fully converted to its Cr(III) form within 12 hours of addition of 4-methoxystyrene. Analysis of the mixture revealed the formation of oxidation products in excess of the amount seen in control experiments (Table 6.3). From those analyses we calculated the total number of turnovers to be 14.78 mol/mol of catalyst. Although this number compares poorly with some of the most efficient iron-based catalysts, it does demonstrate that **7** exhibits some catalytic activity.

The low turnover number suggests that there is significant catalyst deactivation. UV-Vis measurements of the spent solution, however, show that the complex is still intact, but trapped in a Cr^{III} oxidation state.

Measurements via UV-Vis for 5 hours (Figure 6.8) show that there are three distinct phases: rapid establishment of a steady state, a steady state lasting approximately 1 hour, followed by decay to a Cr^{III} state. The non-linearity of the decay strongly suggests product inhibition. Indeed, the final spectrum, while typical of a Cr^{III} corrole species (Q band region), shows a Soret region typical of oxygen-donor ligand, supporting a product inhibition hypothesis.

Conclusion

We have demonstrated that removal of the axial ligands via acid treatment of **8** produces catalytic activity. The turnover number is low and the rate of reaction is slow. Moreover, there is a significant product inhibition. This is, however, the first example of a first row transition metal catalyzing direct O atom transfer from O₂ to substrate, demonstrating again the unusual chemistry of corrole complexes. Major challenges that remain include getting around the inhibition problem as well as the slowness of the reaction. One way to enhance activity could be the use of higher temperatures, coupled with trapping of the product in a form which would not inhibit the reoxidation step. Higher temperatures would also favor dissociation of axial ligands, which could promote reactivity.

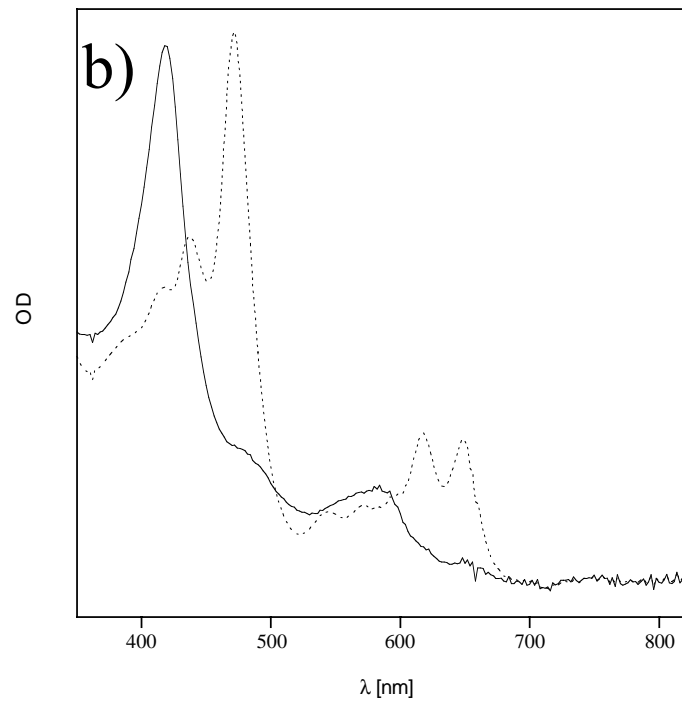
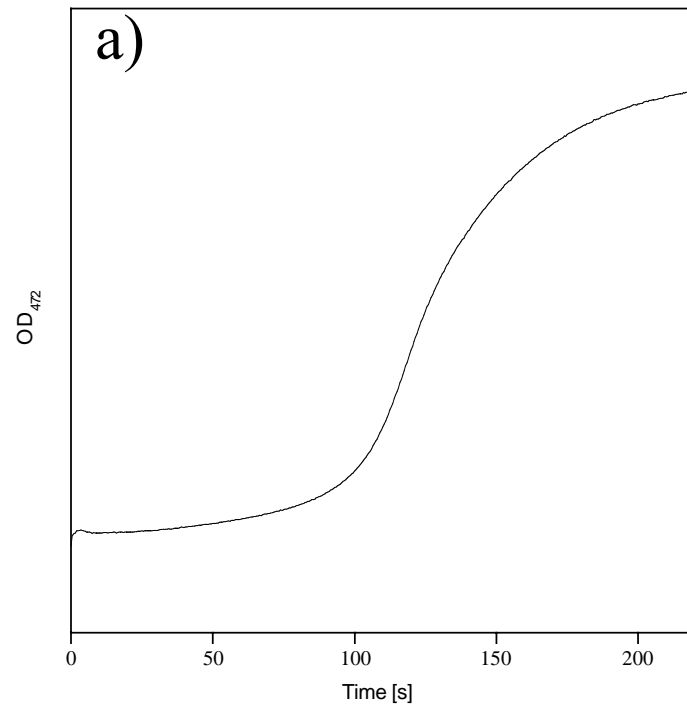
We have also shown that the reactivity of **2** can be significantly increased by bromination of the ligand at β positions. Olefins such as styrene are oxidized by the new compound **7**. The consequences of the increased redox potential are that the air sensitivity of the Cr^{III} state is greatly diminished. It is still unusually high, when compared to porphyrins, since in the latter case, Cr^{III} is not reoxidized by dioxygen. Complex **7** clearly shows that there is no thermodynamic obstacle to O₂ activation and O-atom transfer to olefins by the Cr^VO/Cr^{III} couple when the potential is in a certain region (~600 mV versus Ag/AgCl). The main barrier seems to be kinetic, i.e., the reoxidation step is very slow. The two contributing factors are disfavored ligand dissociation and low reactivity. The latter cannot be overcome without decreasing the O-atom transfer reactivity. However, the position of the ligand dissociation equilibrium can be altered without affecting reactivity and this is worth exploring in the future.

Table 6.3. Products in the aerobic oxidation of 4-methoxystyrene catalyzed by **7**.

	Sample	Control
Styrene oxide Phenylacetaldehyde	10.65 ^a	-----
Benzaldehyde	4.13	1.02

^aall numbers are in mol/mol catalyst. Experimental conditions are 7 0.23 mM, 4-methoxystyrene 250 mM in pentane.

Figure 6.8. a) UV-Vis traces of the reaction between **7** and 4-methoxystyrene over several hours. b) final product.



References

- (1) Samsel, E. G.; Srinivasan, K.; Kochi, J. K. *J. Am. Chem. Soc.* **1985**, *107*, 7606.
- (2) Siddall, T. L.; Miyaura, N.; Huffman, J. C.; Kochi, J. K. *J. Chem. Soc., Chem. Commun.* **1983**, 1185.
- (3) Srinivasan, K.; Kochi, J. K. *Inorg. Chem.* **1985**, *24*, 4671.
- (4) Lyons, J. E.; Ellis Jr., P. E. *Catal. Lett.* **1991**, *8*, 45.
- (5) Ellis Jr., P. E.; Lyons, J. E. *Catal. Lett.* **1989**, *3*, 389.
- (6) Ellis Jr., P. E.; Lyons, J. E. *Coord. Chem. Rev.* **1990**, *105*, 181.
- (7) Grinstaff, M. W.; Hill, M. G.; Labinger, J. A.; Gray, H. B. *Science* **1994**, *264*, 1311.
- (8) Grinstaff, M. W.; Hill, M. G.; Birnbaum, E. R.; Schaefer, W. P.; Labinger, J. A.; Gray, H. B. *Inorg. Chem.* **1995**, *34*, 4896.
- (9) Lyons, J. E.; Ellis Jr., P. E.; Myers, H. K.; Wagner, R. W. *J. Catal.* **1993**, *141*, 311.
- (10) Mahammed, A.; Gray, H. B.; Meier-Callahan, A. E.; Gross, Z. *J. Am. Chem. Soc.* **2003**, *125*, 1162.
- (11) Garrison, J. M.; Ostovic, D.; Bruice, T. C. *J. Am. Chem. Soc.* **1989**, *111*, 4960.
- (12) Garrison, J. M.; Bruice, T. C. *J. Am. Chem. Soc.* **1989**, *111*, 191.

- (13) Meier-Callahan, A. E.; Gray, H. B.; Gross, Z. *Inorg. Chem.* **2000**, *39*, 3605.